

NUCLEAR REACTIONS -- THEORY

Mitsuru Tohyama

We have recently proposed the time-dependent density-matrix theory (TDDM).<sup>1,2</sup> This is a straightforward extension of the time-dependent Hartree-Fock theory (TDHF) to include the effects of two-body collisions. We made the first application of TDDM to fusion reactions of  $^{16}\text{O} + ^{16}\text{O}$ <sup>2</sup> and found that an additional dissipation due to two-body collisions resolved the fusion window anomaly in TDHF.<sup>3</sup> Although TDDM is constructed to describe large amplitude collective motions, we also applied it to small amplitude motions of  $^{16}\text{O}$ <sup>4</sup> to test the theory. We found that TDDM did not bring about the damping of the isoscalar quadrupole motion. In this report we show that higher-order correlations which are neglected in TDDM drastically change the damping rate.

First we present TDDM generalized to include higher-order terms. The new TDDM involves three coupled equations. The first equation determines the single-particle (s.p.) representation. The most convenient s.p. basis  $\psi_\lambda$  may be the solution of a TDHF-like equation

$$i\hbar(\partial/\partial t)\psi_\lambda(r,t) = [-\hbar^2\nabla^2/2M + U(\rho)]\psi_\lambda(r,t) \quad (1)$$

where  $U$  is the self-consistent mean field and is a functional of the one-body density matrix

$$\rho(r,r';t) = \sum_{\lambda\lambda'} n_{\lambda\lambda'}(t)\psi_\lambda(r,t)\psi_{\lambda'}^*(r',t). \quad (2)$$

The second equation is for the occupation matrix  $n_{\lambda\lambda'}$ , of which equation of motion is directly related to the correlated part of the two-body Green's function in equal-time limit<sup>5,6</sup> or the two-body density matrix.<sup>7</sup> In the s.p. representation given by Eq. (1), the equation of motion for  $n_{\lambda\lambda'}$  becomes<sup>5,7</sup>

$$(d/dt)n_{\lambda\lambda'}(t) = (i/\hbar) \sum_{\alpha\beta\gamma} \{ \langle \lambda\gamma | v | \alpha\beta \rangle C_{\alpha\beta\lambda'\gamma}(t) - \langle \alpha\beta | v | \lambda'\gamma \rangle C_{\lambda\gamma\alpha\beta}(t) \} \quad (3)$$

where  $v$  is the residual interaction and  $C_{\alpha\beta\gamma\delta}$  is the correlated part of the two-body density matrix. The third equation of motion in TDDM gives the time evolution of  $C_{\alpha\beta\gamma\delta}$ . The equation of motion for the two-body density matrix, in general, contains a three-body density matrix as well as the one-body density matrix. To close the equation of motion the three-body density matrix is usually replaced by a product of the two-body density-matrix and the one-body matrix. A full presentation of the equation for the two-body density matrix in coordinate space may be seen in Ref. 7. The equation of motion for the two-body density matrix thus obtained contains several terms which represent various two-particle correlations. We take the correlations of two types i.e. the first-order particle-particle correlation and the higher-order particle (p) - hole (h) correlation. The former is included in the original TDDM and the latter, which is responsible for redistribution of 2p-2h level density, is the effect which we investigate in this report. The equation of motion for the two-body density matrix is written as

$$i\hbar \frac{d}{dt} C_{\alpha\beta\gamma\delta}(t) = \sum_{\alpha'\beta'\gamma'\delta'} \langle \alpha'\beta' | v | \gamma'\delta' \rangle \times \{ [\delta_{\alpha\alpha'} n_{\alpha\alpha'}(t)] [\delta_{\beta\beta'} n_{\beta\beta'}(t)] n_{\gamma\gamma'}(t) n_{\delta\delta'}(t) - n_{\alpha\alpha'}(t) n_{\beta\beta'}(t) [\delta_{\gamma\gamma'} n_{\gamma\gamma'}(t)] [\delta_{\delta\delta'} n_{\delta\delta'}(t)] \} \quad (4)$$

$$\begin{aligned}
& + \sum_{\alpha'\beta'\gamma'} \{ \langle \alpha\alpha' | v | \beta'\gamma' \rangle n_{\beta'\gamma'} - \langle \beta'\alpha' | v | \gamma\gamma' \rangle n_{\alpha\beta'} \} C_{\beta'\gamma'\delta\alpha'} \\
& + \sum_{\alpha'\beta'\gamma'} \{ \langle \beta\alpha' | v | \beta'\gamma' \rangle n_{\beta'\delta} - \langle \beta'\alpha' | v | \delta\gamma' \rangle n_{\beta\beta'} \} C_{\alpha\gamma'\gamma\alpha'}
\end{aligned} \quad (4)$$

The first term on the right side is the Born term and Eqs. (1), (3) and (4) with this term are equivalent to the original TDDM. The second and third terms on the right side of Eq. (4) represent higher-order p-h correlations among 2p-2h configurations. For simplicity we neglect exchange terms. The TDDM equations (1), (3) and (4) conserve the total number of particles and the total energy consisting of the Hartree-Fock (HF) energy and the correlation energy<sup>2</sup>: the correlation energy  $E_{\text{cor}}$  is given in terms of the two-body density matrix as

$$E_{\text{cor}} = -(i/2N) \sum_{\alpha\beta\gamma\delta} \langle \alpha\beta | v | \gamma\delta \rangle C_{\gamma\delta\alpha\beta}(t). \quad (5)$$

We study the isoscalar quadrupole motion of  $^{16}\text{O}$ . It is excited by squeezing initially ( $t=0$ ) the Hartree-Fock solution  $\phi_\lambda$  with the quadrupole field as

$$\psi_\lambda(r, t=0) = e^{i\alpha r^2 Y_{20}(\theta)} \phi_\lambda(r), \quad (6)$$

where  $\alpha$  is a parameter determining the amplitude of the oscillation. We use the TDHF code with axial symmetry.<sup>8</sup> The mean potential is calculated with the Bonche-Koonin-Negele force<sup>9</sup> and the s.p. states are taken up to the 2s-1d shell. The 1s and 1p states are assumed to be initially completely occupied and other states totally empty. The two-body density matrix  $C_{\alpha\beta\gamma\delta}$  is assumed to be zero at  $t=0$ . We use a residual interaction of the  $\delta$  function form  $v = v_0 \delta^3(r-r')$ , with  $v_0 = -300 \text{ MeV fm}^3$ . The residual interaction gives the NN cross section of about 40 mb in the Born approximation. The strength  $\alpha$  in Eq. (6) is adjusted to give the mean excitation energy of 22 MeV which is close to the empirical excitation energy of the giant quadrupole resonance.<sup>10</sup> The amplitude of the

motion depends on  $\alpha$  but its time dependence is independent of  $\alpha$  unless  $\alpha$  is very large.

The time evolution of the quadrupole moments is shown in Fig. 1. We compare three different calculations. The dashed curve

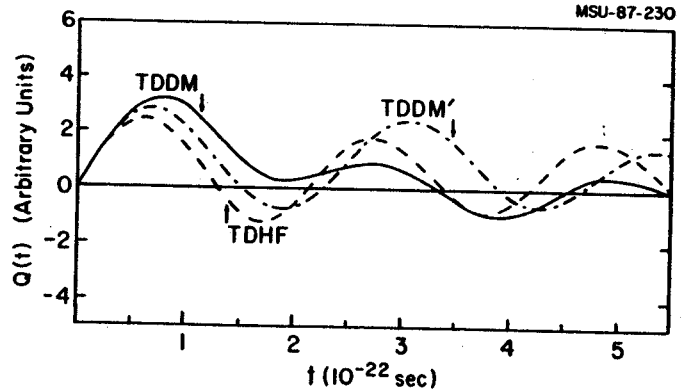


Fig. 1 Time evolution of the isoscalar quadrupole moments calculated in TDHF (dashed curve), in TDDM (solid curve) and in TDDM' (dot-dashed curve) which includes only the Born term.

denotes the TDHF result. The quadrupole moment in TDHF oscillates with a frequency corresponding to the excitation energy of about 20 MeV and the amplitude of the oscillation slightly decays, probably due to particle emission. The dot-dashed curve (referred to as TDDM') shows the TDDM calculation only with the Born term in Eq. (4). This calculation was done with s.p. states up to the 2p-1f shell. The frequency in TDDM' is lowered due to the residual interaction and that the amplitude of the oscillation in TDDM' is slightly larger than that in TDHF is due to an increase in the HF energy associated with the decrease in the correlation energy<sup>2</sup>. As can be seen in Fig. 1, TDDM' brings about no significant damping of the motion, contrary to an expectation from experiment<sup>10</sup> suggesting the life time of about  $10^{-22}$  sec. The result of the full TDDM calculation is shown in Fig. 1 by solid curve. The inclusion of the p-h correlations drastically increases the damping rate of the motion. The relaxation time in TDDM extracted

from the figure is about  $3 \times 10^{-22}$  sec. The correlations play an important role in redistributing the level density of 2p-2h configurations as was the case in shell-model calculations.<sup>11</sup> As a result of these correlations, some of the 2p-2h configurations are shifted to the low frequency region, increasing the level density around the frequency of the isoscalar motion.

In summary, we studied the damping of the isoscalar quadrupole motion of  $^{16}\text{O}$  in TDDM which incorporates particle collision effects into the mean field theory. It is found that the correlations among 2p-2h configurations are important to describe the damping of the motion. It is interesting to study the effects of these higher-order correlations on dissipations and fluctuations in heavy-ion collisions.

---

#### References

1. M. Tohyama, *Phys. Lett.* **163B**,14(1985).
2. M. Tohyama, *Phys. Rev.* **C36**,187(1987).
3. J.W. Negele, *Rev. Mod. Phys.* **54**,913(1982); K.T.R. Davies, K.R.S. Devi, S.E. Koonin, and M.R. Strayer, in *Treatise on Heavy Ion Science*, edited by D.A. Bromley (Plenum, New York 1985), vol. 3.
4. M. Tohyama, to be published.
5. C. Y. Wong and H.H.K. Tang, *Phys. Rev. Lett.* **40**,1070(1978); *Phys. Rev.* **C20**,1419(1979).
6. H. Orland and R. Schaeffer, *Z. Phys.* **A290**,191(1978).
7. S. J. Wang and W. Cassing, *Ann.Phys.(N.Y.)* **159**,328(1985).
8. K.T.R. Davies and S.E. Koonin, *Phys. Rev.* **C23**,2042(1981).
9. P. Bonche, S.E. Koonin and J.W. Negele, *Phys. Rev.* **C13**,1226(1976).
10. F. E. Bertrand, *Ann. Rev. Nucl. Sci.* **26**,457(1976).
11. T. Hoshino and A. Arima, *Phys. Rev. Lett.* **37**,266(1976).

Mitsuru Tohyama

Recent experimental data on subthreshold charged pion production in  $^{139}\text{La} + ^{139}\text{La}$  collisions is quite puzzling<sup>1</sup>. Since there is a neutron excess, one may expect that the production cross section of negative pions is larger than that of positive pions. In fact, an intranuclear cascade calculation for relativistic collisions predicts the  $\pi^-$  to  $\pi^+$  ratio of about 3.<sup>2</sup> In contrast to this expectation, the experiment shows no difference between  $\pi^-$  to  $\pi^+$  cross sections. A statistical model analysis by Bonasera and Bertsch<sup>3</sup> indicates that the Coulomb potential plays a role in reducing the  $\pi^-$  to  $\pi^+$  ratio. We are trying a more microscopic analysis to understand the relative importance of the production mechanism, the heavy-ion collision dynamics and pion rescatterings. To obtain pion yields at the production stage we used the first chance nucleon-nucleon collision model.<sup>4</sup> In this model the phase space distribution of nucleons is approximated by two separated Fermi spheres and the production rate is given as

$$\begin{aligned} \frac{d^5N}{d^3p dt dV} &= \frac{1}{(2\pi)^3 2\omega} \int d^3p_1 d^3p_2 d^3p_3 d^3p_4 \\ &\times 2\pi\delta(E)(2\pi)^3 \delta^3(p) f_1 f_2 (1-f_3)(1-f_4) \\ &\times |\langle pp_3 p_4 | T | p_1 p_2 \rangle|^2 \end{aligned} \quad (1)$$

where  $f$  is the occupation factor and  $T$  is the  $t$  matrix for the elementary process  $NN \rightarrow NN\pi$ . We calculated  $T$  in the Born approximation for a  $\Delta$  excitation model. The parameters of the model were adjusted to fit existing  $NN \rightarrow NN\pi$  data. The dominant channel of  $\pi^+$  production is  $p+p \rightarrow p+n+\pi^+$  and that of  $\pi^-$  production  $n+n \rightarrow n+p+\pi^-$ . Since the number of protons differs from that of neutrons, we used different Fermi momenta for protons and

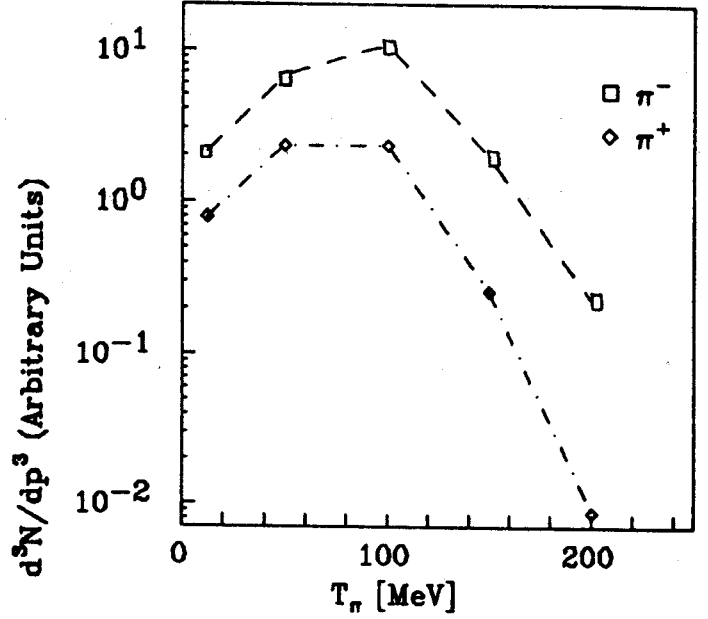


Fig. 1 Pion c.m. spectra from the La+La collision at  $E_{\text{lab}}/\text{nucleon} = 246\text{MeV}$  calculated in the first NN collision model.

neutrons. The pion spectra at  $E_{\text{lab}}/\text{nucleon} = 246\text{ MeV}$  are shown in Fig. 1 as a function of pion c.m. kinetic energy. In the low energy region of the spectra the  $\pi^-$  to  $\pi^+$  ratio is close to the ratio of the number of neutron pairs to that of proton pairs  $(N \times N / Z \times Z) = (82/57)^2 = 2.1$ . However, with increasing pion energy the ratio becomes larger. This is due to the larger neutron Fermi sphere. The Pauli blocking factor  $f_1 f_2 (1-f_3)(1-f_4)$  does not affect the  $\pi^-$  to  $\pi^+$  ratio at this incident energy.

The pion production cross section is modified if there is a difference between the proton and neutron potentials. To get information about the time evolution of the mean field, we performed a dynamical calculation of La+La collision based on the BUU model.<sup>5</sup> The distributions of the mean fields in the early stage of the collision look as follows: The Coulomb potential is nearly doubled. However,

in the high density region (around the c.m.) where most pions are considered to be created the increase in the Coulomb energy is almost canceled by that of the symmetry energy, resulting in a small difference between the proton and neutron potentials there. Therefore the  $\pi^-$  to  $\pi^+$  ratio obtained from Eq. (1) would not be strongly modified by the mean fields.

If we assume that a pion is absorbed by two nucleons, the dominant channel is  $\pi^- + n + p \rightarrow n + n$  for  $\pi^-$  and  $\pi^+ + n + p \rightarrow p + p$  for  $\pi^+$ . Since there is a large difference between the proton and neutron potential outside the high density region, the absorption rate depends on the charge state of a pion:  $\pi^-$  absorption is favored because the Coulomb energy is released in the  $\pi^- + n + p \rightarrow n + n$  process. The ratio of pion mean free path may be expressed by the ratio of final level densities as  $\lambda_{\pi^-} / \lambda_{\pi^+} = \exp(-2(\mu_p - \mu_n)/T)$  where  $\mu_p$  ( $\mu_n$ ) is the chemical potential for protons (neutrons) and the  $T$  is the temperature at which a pion is absorbed. Assuming that a pion travels about 6 fm in the nuclear medium, and taking  $\mu_p - \mu_n = 15$  MeV and  $T = 29$  MeV<sup>1</sup>, we find that the ratio of the absorption rate is about 6, which seems to explain the difference between the result from Eq. (1) and the experiment. A dynamical model such as that used by Bauer et al.<sup>6</sup> for photon production might be useful to get a more quantitative understanding.

---

#### References

1. J. Miller et al., Phys. Rev. Lett. 58, 2408 (1987).
2. Y. Kitazoe et al., Phys. Rev. Lett. 58, 1508 (1987).
3. A. Bonasera and G. Bertsch, Phys. Lett. 195B, 521 (1987).
4. G. Bertsch, Phys. Rev. C15, 713 (1977).
5. G. Bertsch et al., Phys. Rev. C29, 673 (1984).
6. W. Bauer et al., Phys. Rev. C34, 2127 (1986).

G. Bertsch and M. Gong

In collaboration with L. McLerran, V. Ruuskanen, and E. Sarkkinen,<sup>1</sup> we have developed a cascade code to simulate the hadronization of a QCD plasma phase which may be formed in ultrarelativistic heavy ion collisions. The code handles the propagation of the pions and their mutual scattering in the same way as was done in earlier cascade codes to simulate the evolution of nucleon distributions. The pi-pi scattering cross section is deduced from phase shift analyses.

A key new ingredient in the model is the treatment of the phase transition from the plasma phase to the hadronic phase. Our model is analogous to the Weisskopf model of compound nucleus evaporation. Globes of plasma evaporate pions from their surfaces, just as hot nuclei evaporate neutrons. The rates are determined by detailed balance, assuming that the globes are completely absorbing.

An important motivation for this work is to test the validity of approximations made in previous hydrodynamic studies.<sup>2</sup> Our study led to the following conclusions:

1. The one-dimension hydrodynamic model, assuming a purely longitudinal expansion, is useful only for collisions with relatively low  $dN/dy$ . For  $dN/dy$  greater than  $4A$ , the transverse expansion governs the duration of the plasma phase, decreasing its duration.
2. There is very little transverse expansion of the plasma, in qualitative agreement with the three-dimensional hydrodynamic models that predict an inward-propagating rarefaction shock having pure hadronic matter on the downstream side. The pion distribution halfway through the hadronization agrees quite well with the three-dimensional hydrodynamic calculation.

3. The pions hardly interact with each other in the final state. For example, at a particle density  $dN/dy=4A$ , the average number of collisions undergone by a final state pion is 1.8. The rapid freezeout means that the final state essentially preserves a view of the surface of the plasma phase.
4. The cascade confirms a prediction of the 3-D hydrodynamics calculations, that the mean transverse momentum in the final state,  $\langle p_{\text{perp}} \rangle$ , has a flat dependence on  $dN/dy$  when there is a plasma phase transition. This is an obvious consequence of the behavior in (3) above.

---

#### References

1. G. Bertsch, M. Gong, L. McLerran, V. Ruuskanen and E. Sarkkinen, Phys. Rev. D, to be published.
2. H. von Gersdorff, et al., Phys. Rev. D34, 794(1986); M. Kataja, et al., Phys. Rev. D34, 2755(1986).

G. Bertsch, M. Gong and M. Tohyama

We are studying the correlations between pions produced in ultrarelativistic heavy ion collisions, using a cascade model of the collisions that we recently developed.<sup>1</sup> These correlations are sensitive to the spatial and temporal characteristics of the collision process as in Hanbury-Brown and Twiss interferometry. The correlation function between pions of four-momentum  $p$  and  $p'$  is defined

$$R(p,p') = \frac{d^6 n/d^3 p d^3 p'}{\left(\frac{d^3 n}{d^3 p}\right) \left(\frac{d^3 n}{d^3 p'}\right)} \quad (1)$$

The theory assumes that the pions are produced by an incoherent source function  $g(p,x)$ . Then the correlation is calculated as

$$R(p,p') = 1 + \frac{\int d^4 x d^4 x' g(\vec{p},x) g(\vec{p}',x') \cos \Delta p \cdot \Delta x}{\int d^4 x g(p,x) \int d^4 x g(p',x)} \quad (2)$$

The source function is obtained from the cascade calculation by the expression

$$g(p,x) = \sum_i^N \int d^3 p' \delta^{(4)}(x-x_i) \delta^{(4)}(p-p_i) e^{-\frac{(p-p')^2}{p_0^2}}$$

The sum ranges over final state pions. The  $p_i$  and  $x_i$  are the coordinates of the pions at their point of last interaction. The cascade distribution is smoothed using a gaussian, with parameter  $p_0 = 120$  MeV/c. In addition, we summed over a number of cascade runs to generate enough points for a smooth distribution.

We have studied the source function for a collision in which the initial geometry is a cylinder of plasma of radius 3 fm, and with an energy density giving  $dn/dy = 80$  in the final state. We found that the source can be quite well described by the function

$$g(p,x) = f(p_{\text{perp}}) \tau \exp\left[-\left(\frac{t}{\tau_0}\right)^2 - \left(\frac{r_{\text{perp}}}{R}\right)^2 - \left(\frac{y_x - y_p}{y_0}\right)^2\right] \quad (3)$$

$$\begin{aligned} \text{with } \tau_0 &= 9 \text{ fm/c} \\ R &= 3.3 \text{ fm} \\ y_0 &= 0.76. \end{aligned}$$

Here  $\tau = \sqrt{t^2 - z^2}$  is the proper time of the source, and  $y_x, y_p$  are the rapidities associated with the four-vectors  $x, p$ . The dependence of the source on  $p_{\text{perp}}$ , given by the function  $f$ , is irrelevant for our purposes. One interesting point to note, is that because the time duration is longer than the spatial size of the source, the correlation in the outward direction will be sensitive to the temporal properties of the source.

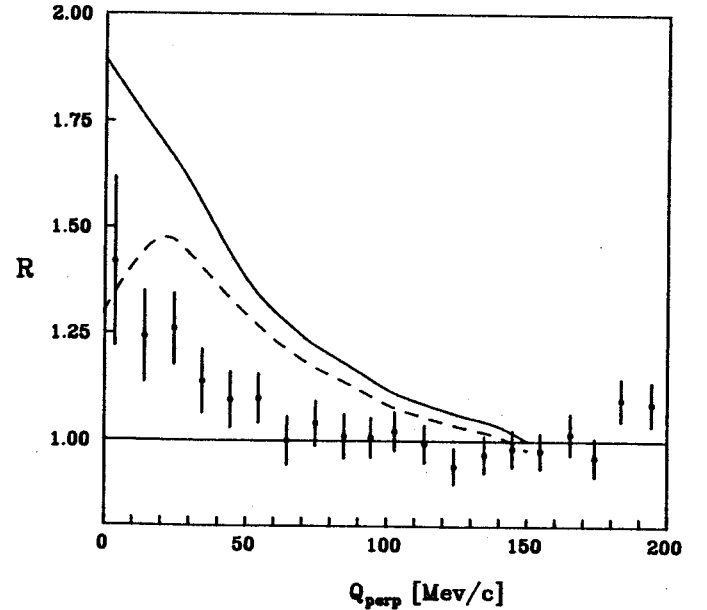


Fig. 1 Correlation function  $R$  between pions in 200 GeV/c  $^{16}\text{O}$  collisions with  $^{208}\text{Pb}$ . The pions are selected with rapidity  $2 < \eta < 3$ , and relative longitudinal momentum  $|Q_{\text{perp}}| < 100$  MeV/c. Solid line is the result of the cascade simulation, Eq. (2). The dashed line is corrected for the Coulomb repulsion between pions. Data points are from Ref. 2.



Figure 1 shows the predicted correlation function compared with recent data from the NA35 experimental at CERN.<sup>2</sup> The solid lines shows the predicted R from Eq. (2) integrating over the same ranges of momentum as reported in the experiment. The dashed curve is corrected for the  $\pi$ - $\pi$  Coulomb interaction by the factor  $2\pi\eta/(e^{2\pi\eta}-1)$ .

---

#### References

1. See previous contribution.
2. T. Humanic, "Pion Interferometry with Ultra-relativistic Heavy-Ion Collisions from NA35 Experiment", Quark Matter 1987 Conference, Nordkirchen, West Germany.

A. Bonasera and L.P. Csernai

The collective fluid dynamical flow is one of the major discoveries in high energy heavy ion physics.<sup>1</sup> A lot of experimental data have been collected in the last few years using different experimental techniques,<sup>2-9</sup> and by now the majority of the data is analyzed using the powerful method first proposed by Danielewicz and Odyniecz.<sup>2</sup> To compare the large number of different experimental results with various energies and masses seems to be a difficult task. However, the general features of the collective flow could, in principle, be expressed in terms of scale invariant quantities as was pointed out in Ref. 10. In this way the particular differences arising from the different initial conditions, masses, energies etc., can be separated from the general fluid dynamical features. Theoretical fluid dynamical calculations predicted the collective flow long ago.<sup>11-13</sup> If perfect fluid dynamics is applicable under the conditions discussed in Ref. 10, then a scale invariant representation of the data would eliminate the differences among the results. Deviations from such an ideal scaling signal physical processes which lead to a not scale invariant flow, like special properties of the equation of state (EOS), potential energy, or phase transitions, dissipation, relativistic effects, etc.

In order to investigate the validity of our scaling assumption, we first express measured quantities in a scale invariant way. We introduce a scale invariant transverse momentum per nucleon

$$\tilde{p}^x = p^x / p_{proj}^{CM}$$

where  $p^x$  is the transverse momentum per nucleon obtained in the experiments and  $p_{proj}^{CM}$  is the Center of Mass momentum of a nucleon in the

projectile. In the same way we define the scale invariant rapidity by

$$\tilde{y} = y^{CM} / y_{proj}^{CM}$$

We use the definition introduced in Ref. 3 to characterize the transverse momentum dependence by one quantity: the slope of the rapidity dependence of the transverse momentum near mid-rapidity. This parameter was named "Flow" in Ref. 3. We denote the corresponding scale invariant slope by  $\tilde{F}$ .

The scale invariant transverse momenta show a general feature. Deviations from a constant  $\tilde{F}$  indicate deviations from the perfect scale invariant fluid flow. There are two main reasons for such deviations: the viscous dissipation and the nonscaling behavior of the EOS. Let us first study the effects of the viscosity. Viscous flow patterns are similar to each other if their respective Reynolds numbers,  $Re$ , are the same, as described in Ref. 10. We can calculate  $Re$  by using the temperature and density dependence of the viscosity  $\eta$ .<sup>14</sup>

If we display the contour lines of constant  $\tilde{F}$  on the same plot, at medium and high energies the qualitative behavior of the contour lines is similar. The experimental data, however, rise somewhat sharper than the Reynolds number. This most probably indicates that the viscosity increases faster with energy than  $\sqrt{E_{nucl}^{CM}}$  or  $\sqrt{T}$  calculated in Ref. 17, because of other inelastic processes, pion emission etc. The same processes may also lead to a softening of the EOS which will result in smaller transverse flow. Also, at high beam energies a partial transparency is expected to occur which can reduce the transverse flow.

The most drastic difference between the  $Re=const.$  and  $\tilde{F}=const.$  curves appears at low

energies. Below  $E_{\text{nucl}}^{\text{CM}} \approx 60-70$  MeV the scale invariant transverse flow  $\tilde{F}$  drops suddenly with decreasing energy, and below  $E_{\text{nucl}}^{\text{CM}} \approx 10$  MeV it becomes negative according to recent experimental data<sup>7,9</sup> for asymmetric systems. The deflection angle (and therefore  $\tilde{F}$ ) of the emitted particles is "negative", i.e. the projectile is deflected to the target side in non-central collisions. The Reynolds number decreases also, but this decrease starts at lower energy  $E_{\text{nucl}}^{\text{CM}} \approx 50$  MeV, and it never changes sign! The observed behavior is certainly unexplainable by minor changes in the viscosity. A sufficiently strong attractive mean field leads to an EOS showing a first order, liquid-gas type phase transition. Thus either the EOS or the reaction mechanism should change here drastically. The EOS enters the scaling analysis via the sound speed. Using an EOS with binding energy 8 MeV and  $K=250$  MeV the sound speed is constant,  $\tilde{c}_s = 0.7-0.9$  for  $n=0.3-1.0$  and  $E_0=50-240$  MeV ( $T=35-160$  MeV). Below  $E_0=40$  MeV  $\tilde{c}_s$  starts to diverge with decreasing energy: at  $\tilde{n}=1$   $\tilde{c}_s \gg 1$ , at  $\tilde{n}=0.6$   $\tilde{c}_s = 0.7$ , and at  $\tilde{n}=0.3$   $\tilde{c}_s \rightarrow 0$ . This nonscaling behavior of  $\tilde{c}_s$  at low energies is related to the liquid-gas phase transition of our EOS. The two effects, the softening of the EOS or the negative pressure caused by the nuclear liquid-gas phase transition, and the predominance of the nuclear attractive mean field (or surface tension) are, of course, the two sides of the same microscopic attractive nucleon-nucleon interaction.

This contribution is based on Ref. 15.

## References

1. H.A. Gustafsson, et al., Phys. Rev. Lett. 52,1590(1984) .
2. P. Danielewicz and G. Odyniecz, Phys. Lett. 157B,146(1985).
3. K.G.R. Doss, et al., Phys. Rev. Lett. 57, 302(1986); H.G. Ritter, et al., Nucl. Phys. A447,3c(1985).
4. A. Sandoval, et al., GSI scientific report 1985, pg. 97, and Phys. Rev. Lett. 53,763 (1984).
5. P. Beckmann, et al., GSI Scientific Report 1985, pg. 98.
6. L.P. Csernai, et al., Phys. Rev. C34,1270 (1986).
7. M.B. Tsang, et al., Phys. Rev. Lett. 57, 559(1986).
8. D. Beavis, et al., Phys. Rev. C33,1113 (1986).
9. F. Deák, et al., Nucl. Phys. A464,133 (1987).
10. N. Balázs, B. Schürmann, K. Dietrich and L.P. Csernai, Nucl. Phys. A424,605(1984).
11. W. Scheid, H. Müller, W. Greiner, Phys. Rev. Lett. 32,741(1974).
12. G.F. Chapline, M.H. Johnson, E. Teller, M.S. Weiss, Phys. Rev. D8,4302(1973).
13. H. Stöcker, et al., Phys. Rev. Lett. 47, 1807(1981).
14. P. Danielewicz, Phys. Lett. 146B, 168 (1984).
15. A. Bonasera, L.P. Csernai, Phys. Rev. Lett. 59,630(1987).

L.P. Csernai

The theory of shock waves in relativistic fluid dynamics<sup>1</sup> has proven its importance through a number of elegant applications in cosmology<sup>2-5</sup> and, more recently, in relativistic heavy ion reactions.<sup>6-10</sup> Usually a shock wave is formed when matter is compressed very rapidly by an external force. Shock-like discontinuities would also be formed spontaneously when a system undergoes a first order phase transition during the expansion stage.<sup>11</sup> In all these cases, shock waves propagate with a velocity smaller than the light velocity. Therefore the world sheet swept out by the surface of the shock front draws a space-like hypersurface in the Minkowski space. The conservation laws across this surface lead to the Rankine-Hugoniot-Taub equation, which relates the fluid variables (e.g. pressure, fluid velocity, conserved charge density) on the two sides of the shock front.

Recently it was pointed out<sup>12</sup> that under certain conditions the system may undergo a rapid bulk phase transition through a timelike surface of discontinuity. This happens when the system is diluted very rapidly and uniformly and the nucleation of bubbles occurs at many spatially adjacent points which are not causally connected to each other. An example of this is the inflationary universe scenario. In this case, the spacelike phase boundary, if it is smoothed out, becomes a timelike surface  $\Sigma$ . The thickness  $\tau$  of this transition zone would be determined by the bubble formation rate and the velocity of bubble growth. If  $\tau$  is small enough compared with the characteristic time scale of the processes of interest, one may consider the phase transition as taking place through a structureless timelike surface. The purpose of this note is to give a general derivation of the Rankine-Hugoniot-Taub equation which is

applicable both for the spacelike surface and the timelike surface of shock discontinuity. Let us denote the normal vector of the surface  $\Sigma$  by  $\Lambda^\mu$ . Then from the normalization:

$$\Lambda_\mu \Lambda^\mu = \begin{cases} +1 & \text{timelike surface} \\ -1 & \text{spacelike surface} \end{cases} \quad (1)$$

The physical state of the system can be characterized by the energy momentum tensor:

$$T^{\mu\nu} = w u^\mu u^\nu - p g^{\mu\nu}, \quad (2)$$

where the enthalpy density,  $w = e + p$ , is the sum of the energy density,  $e$ , and pressure,  $p$ ,  $u^\mu = (\gamma, \gamma v)$  is the four fluid velocity, normalized to  $u^\mu u_\mu = 1$  and  $g^{\mu\nu} = \text{diag}(1, -1, -1, -1)$  is the metric tensor. If we have a discontinuity across the surface, we can label any given fluid dynamical quantity, say  $Q$ , on one side of the surface by the index "1" ( $Q_1$ ) and on the other side by "2" (i.e.  $Q_2$ ). Then the change of this quantity will be represented by

$$[Q] = Q_2 - Q_1 \quad (3)$$

Using this notation the conservation laws across the surface of the discontinuity take the form:

$$[R^\mu] = [T_{\mu\nu} \Lambda^\nu] = 0, \quad (4)$$

(energy and momentum conservation)

$$[j] = [n^\mu \Lambda_\mu] = 0, \quad (5)$$

(conservation of particle number). Eq. (5) can be written for any independently conserved charge with the four current of the conserved charge. We can introduce an invariant scalar

proper density  $n = n^\mu u_\mu$  assuming that the flow is coupled to the conserved charge, and a quantity  $x = w/n^2$ , which plays the same role as the specific volume  $V$  in the nonrelativistic theory. In fact,  $x \rightarrow mV$  in the nonrelativistic limit ( $m$  is the particle mass).

In order to derive the equation of the detonation adiabat (which depends on thermodynamic quantities only) we have to eliminate the four velocity from Eqs. (4) and (5). Since Eq. (4) is a vector equation we can cast it into two independent equations by taking its projection into the normal direction of the surface  $\Sigma$

$$[R^\mu]_{\Lambda_\mu} = 0, \quad (6)$$

and projecting it into the surface by the projector  $P^{\mu\nu} = g^{\mu\nu} - \Lambda^\mu \Lambda^\nu / (\Lambda_\alpha \Lambda^\alpha)$ :

$$[G^\mu] = [P^{\mu\nu} R_\nu] = 0 \quad (7)$$

Eq. (7) can be split into a scalar equation showing that the length of the vector  $G$  is conserved

$$[G_\mu \cdot G^\mu] = 0, \quad (8)$$

and into an equation which requires the direction of the projection  $G^\mu$  be unchanged,  $[G^\mu / |G^\mu|] = 0$ . After straightforward calculation from Eqs. (5) and (6) we find that the current  $j$  across the surface satisfies

$$j^2 = [p] (\Lambda^\mu \Lambda_\mu) / [x] \quad (9)$$

Also, from Eqs. (5) and (8), we obtain

$$j^2 = [wx] / [x^2] (\Lambda_\mu \Lambda^\mu) \quad (10)$$

From the above two relations we can get immediately the equation of the Taub adiabat

$$[p] (x_1 + x_2) = [wx] \quad (11)$$

in its already well known form. For given  $p_1$  and  $x_1$ , this equation determines the relation between  $p_2$  and  $x_2$ , if the equation of state is known. We note here that the normal vector of the surface  $\Lambda^\mu$  entered in this equation only through  $(\Lambda_\mu \Lambda^\mu)^2$ , which is equal to 1 and hence dropped out! Thus the equation of the Taub adiabat is the same for spacelike and timelike surfaces of discontinuity. Yet, there exists an essential difference between timelike and spacelike surfaces of discontinuities.

Summarizing these results it can be emphasized that using a general derivation for a discontinuity across an arbitrary surface in relativistic fluid flow we succeeded in extending the Rankine-Hugoniot-Taub equations into a new region not discussed before. This region was even considered being unphysical based on nonrelativistic analogies. The introduction of the concept of timelike detonations completes the relativistic theory of rapid combustion and condensation phenomena. This contribution is based on Ref. 14.

#### References

1. A.H. Taub, Phys. Rev. 74, 328(1948).
2. K.S. Thorne, Astrophys. J. 179, 897(1973).
3. P.J. Steinhardt, Phys. Rev. D25, 2074 (1982).
4. M.H. Johnson and C.F. McKee, Phys. Rev. D3, 858(1971).
5. G. Lasher, Phys. Rev. Lett. 42, 1646(1979); A.H. Guth, E.J. Weinberg, Phys. Rev. D23, 876(1981).
6. E.V. Shuryak, Phys. Reports 61, 71(1980).
7. C. Van Hove, Z. Phys. C21, 93(1983).
8. B.L. Friman, G. Baym and J.-P. Blaizot, Phys. Lett. 132B, 291(1983).
9. M. Gyulassy, K. Kajantie, H. Kurki-Suonio and L. McLerran, Nucl. Phys. B237, 477 (1984).
10. L.P. Csernai, Phys. Rev. D29, 1945(1984).
11. L.P. Csernai and M. Gong, Phys. Rev. D (1988) in press.
12. N.K. Glendenning and T. Matsui, Phys. Lett. 141B, 419(1984).
13. L.D. Landau and E.M. Lifshitz, Fluid-Mechanics (Pergamon, 1959).
14. L.P. Csernai, Sov. JETP 92, 213(1987).